Biophysical Journal Volume 71 August 1996 778–786

Circular Dichroism Studies of the Mitochondrial Channel, VDAC, from *Neurospora crassa*

Ling Shao,*# Kathleen W. Kinnally,*§ and Carmen A. Mannella*#§

*Division of Molecular Medicine, the Wadsworth Center; and #Department of Physics and §Department of Biomedical Sciences, The University at Albany, State University of New York, Albany, New York 12201 USA

ABSTRACT The protein that forms the voltage-gated channel VDAC (or mitochondrial porin) has been purified from *Neurospora crassa*. At room temperature and pH 7, the circular dichroism (CD) spectrum of VDAC suspended in octyl β-glucoside is similar to those of bacterial porins, consistent with a high β-sheet content. When VDAC is reconstituted into phospholipid liposomes at pH 7, a similar CD spectrum is obtained and the liposomes are rendered permeable to sucrose. Heating VDAC in octyl β-glucoside or in liposomes results in thermal denaturation. The CD spectrum irreversibly changes to one consistent with total loss of β-sheet content, and VDAC-containing liposomes irreversibly lose sucrose permeability. When VDAC is suspended at room temperature in octyl β-glucoside at pH <5 or in sodium dodecyl sulfate at pH 7, its CD spectrum is consistent with partial loss of β-sheet content. The sucrose permeability of VDAC-containing liposomes is decreased at low pH and restored at pH 7. Similarly, the pH-dependent changes in the CD spectrum of VDAC suspended in octyl β-glucoside also are reversible. These results suggest that VDAC undergoes a reversible conformational change at low pH involving reduced β-sheet content and loss of pore-forming activity.

INTRODUCTION

A voltage-dependent anion-selective channel, VDAC, is a major protein component in the mitochondrial outer membrane, probably forming the main pathway for the movement of ions and metabolites across this membrane (Colombini, 1979). Electron microscopic studies of two-dimensional crystals of fungal VDAC indicate that the pore diameter is 2.5–3 nm (Mannella et al., 1989; Guo et al., 1995), consistent with the functional properties of the open channel (Mannella et al., 1992; Colombini, 1994). When it is reconstituted in planar bilayers, VDAC usually occupies its fully open state at small transmembrane potentials and switches to lower-conductance substates when potentials exceed 20–30 mV in either direction. The conductance transitions usually observed correspond to partial (approximately two-thirds) closure of the pore. There are several indications that the less-permeable substates of VDAC may be physiologically relevant. In particular, gating properties are highly conserved and are modulated by endogenous mitochondrial components, NADH (Zizi et al., 1994) and a protein fraction isolated from the space between the inner and outer membranes (Holden and Colombini, 1993). The voltage dependence of the channel is also affected by pH (Bowen et al., 1985; Mirzabekov and Ermishkin, 1989), group III metal hydroxides (e.g., aluminum; Dill et al., 1987), and anionic polymers (Colombini et al., 1987). Incubation of isolated mitochondria with one such polyanion has been shown to diminish ATP uptake by mitochondria (Benz et al., 1988) and VDAC-containing liposomes (Colombini et al., 1987), suggesting that VDAC may regulate the mitochondrial influx and efflux of important metabolites.

The VDAC channel is formed by a single copy of a polypeptide of ~280 amino acids that is encoded by nuclear DNA and synthesized on cytoplasmic ribosomes. VDAC apparently binds to a protease-sensitive receptor on the outer mitochondrial membrane (Pfaller and Neupert, 1987), but little is known about subsequent steps of membrane insertion and pore formation. The occurrence in the VDAC polypeptide of numerous segments of alternating polar–nonpolar residues led Forte et al. (1987) to propose that the polypeptide might fold as an amphiphilic β-sheet. If the β-sheet is twisted into a cylinder, the resulting β-barrel could form a pore with a hydrophilic inner lumen and a lipophilic exterior. The existence of β-barrel pores was confirmed several years later by x-ray crystallography of bacterial porins (Weiss et al., 1990; Cowan et al., 1992), a class of proteins in the outer envelopes of gram-negative bacteria that, like VDAC, form large-conductance ion channels. In fact, VDAC is commonly referred to as a mitochondrial porin, despite the absence of overall sequence homology with bacterial porins. Mannella et al. (1996) recently demonstrated that amino acid sequences of VDAC from different species contain numerous matches with a short (11-residue) motif found by the Gibbs sampler to correspond to transmembrane β-strands in bacterial porins (Neuwald et al., 1995). Images of fungal VDAC provided by electron crystallography (Mannella et al., 1989; Guo et al., 1995) are consistent with a β-barrel slightly wider than that of bacterial porin but have insufficient resolution to distinguish secondary structure.

Received for publication 13 February 1996 and in final form 26 April 1996.

Address reprint requests to Dr. Carmen A. Mannella, Wadsworth Center, New York State Department of Health, Empire State Plaza Box 509, Albany, NY 12201-0509. Tel.:518-474-2462; Fax: 518-486-4901; E-mail: carmen@wadsworth.org

0006-3495/96/08/778/09 $2.00

Here the circular dichroism (CD) spectra of purified fungal VDAC in detergent suspension are reported and compared with those of bacterial porins. Correlations are drawn between changes in the CD spectrum of detergent-solubilized VDAC and in the pore-forming activity of VDAC reconstituted in liposomes that are induced by varying temperature and pH. The results provide the first direct experimental information about the secondary structure of this pore-forming protein and indicate that the protein undergoes a reversible conformational change at low pH.

MATERIALS AND METHODS

Materials

Hydroxylapatite (fast flow), lauryl dimethylamine oxide (LDAO), octyl β-glucoside (β-OG), and egg yolk L-α phosphatidyl choline were obtained from Calbiochem (La Jolla, CA), and egg lectin phosphatidic acid from Avanti Polar Lipids, Inc. (Alabaster, AL). All other chemicals were obtained from Sigma Chemical Co. (St. Louis, MO). Solutions were made with deionized water (Milli-Q system, Millipore Corp., Bedford, MA).

Purification of VDAC

Mitochondria were isolated from liquid cultures of wall-less *Neurospora crassa* protoplasts (FGSC 326) by procedures described by Mannella (1982). The protocol for purification of VDAC from these mitochondria (described in the next paragraph) is based on one developed for bovine-heart mitochondria by De Pinto et al. (1989). Protein concentrations of mitochondrial suspensions were measured by the BCA method (Pierce, Rockford, IL) with 0.2% β-OG or 0.1% LDAO and with bovine serum albumin as the standard. All steps were done at 4° unless otherwise indicated.

Twenty volumes of 2X Buffer A (4% LDAO, 20 mM Tris·HCl, 2 mM sodium EDTA, pH 7.0) were added slowly with continuous stirring to a suspension of *N. crassa* mitochondria containing 15-mg mitochondrial protein/mL of isolation medium, up to a total of 30 mg mitochondrial protein. The clarified mitochondrial suspension was stirred gently for 30 min and centrifuged at 15,000 rev/min for 1 h in an SS34 rotor (Beckman Instruments, Palo Alto, CA). The supernatant, which contained the bulk of the mitochondrial protein, was reduced to 10-mL maximum volume (as needed) by centrifugation in a Centricon 30 tube (Amicon, Beverly, MA) and loaded on a 16-mm-diameter column containing 9 g of a 2:1 mixture of hydroxylapatite/celite, prewashed with Buffer A. After loading, the column was washed extensively with Buffer A, and VDAC was eluted with Buffer A containing 50 mM KCl. Procedures were done on a Waters model 650 Advanced Protein Purification System (Millipore Corp.), and a Lambda-Max model 481 spectrophotometer (Millipore Corp.) was used to monitor A_{280} during elution.

Eluted VDAC fractions were pooled (total volume 7.5–10 mL), concentrated by centrifugation in Centricon 30 tubes to a volume of ~1 mL (containing typically 50–250 μg protein/mL), and stored at −20°. For detergent exchange, the protein in aliquots of this suspension was precipitated by slowly adding 5 volumes acetone (−20°), gently shaking for 1 h, and centrifuging for 30 min at 14,000 × *g* (Model 5402 microfuge, Brinkman Instruments, Westbury, NY). The protein pellet was washed with 1-mL cold acetone, repelleted, and resuspended in appropriate detergent-containing buffers. Residual acetone was evaporated by gently shaking the open tubes for 1 h.

Gel electrophoresis and western blotting

Protein fractions were precipitated with cold acetone (as above) and electrophoresed on 13.5% polyacrylamide slab gels by use of buffers containing 1% sodium dodecyl sulfate (SDS) (Laemmli, 1970) with the Mini-Protean II system (Bio-Rad Laboratories, Hercules, CA). The proteins in the gels were either visualized by silver staining (Bio-Rad) or electrotransferred with the Mini-Trans-Blot system (Bio-Rad) to nitrocellulose membranes (0.45 μm, Bio-Rad). Electrotransfer and immunoblotting were done as described by Stanley et al. (1995) using antibodies directed against residues 1–20 of fungal VDAC, provided by S. Stanley of the Division of Molecular Medicine, the Wadsworth Center, Albany, NY.

Amino-acid composition and protein determination

Purified VDAC (13.5 μg) in TE buffer (10 mM Tris, 1 mM sodium EDTA, pH 7.0) containing 2% β-OG (2% β-OG/TE) was acid hydrolyzed, and its amino-acid composition was determined by the Wadsworth Center's Protein Biochemistry Core Facility by use of a Beckman System Gold analyzer. A molecular weight of 29,979 (Kleene et al., 1987) was used to determine amino acid stoichiometries. The concentrations of two pure VDAC fractions obtained from amino-acid analysis as described above were used as references to calibrate the absorbance of VDAC in 2% β-OG/TE in the wavelength range 184–260 nm. Ultraviolet absorbance spectra were subsequently used to determine the concentrations of VDAC in similar suspensions.

Reconstitution of VDAC into phospholipid vesicles

VDAC was reconstituted into small unilamellar vesicles (SUVs) by modifications of freeze–thawing procedures described elsewhere (Colombini, 1980; Bathori et al., 1993). Phospholipids (36 mg egg yolk L-α phosphatidyl choline and 4 mg egg lectin phosphatidic acid in chloroform) were vortexed, coated onto a glass tube, and dried under nitrogen for 1 h. After resuspension in 1-mL TE buffer and a few minutes of vortexing, the suspension was sonicated to clarity (10–20 min, Ultrasonic cleaner, Bransonic Ultrasonics Corp., Danbury, CT) to yield the stock SUV suspension. Three types of VDAC-reconstituted liposome were made from this stock SUV suspension for different applications:

Type A liposomes (swelling assays): An aliquot of the stock SUV suspension was mixed with 12 volumes of 1% β-OG/TE and 2 volumes of a suspension of 20 μg/mL VDAC in 2% β-OG/TE. The resulting suspension was diluted with 3 volumes of the stock SUV suspension and subjected to three rapid cycles of freeze–thawing (with dry ice/alcohol). The resulting cloudy, viscous suspension contained 30 mg/mL phospholipid, 0.60 μg/mL VDAC (i.e., 20 ng VDAC/mg lipid), and 0.27% β-OG. Variations in this procedure included decreasing the final VDAC concentration (to 0.3–0 μg/mL) and using detergents other than β-OG (LDAO, SDS, or Triton X-100). Other controls involved using bovine serum albumin (final concentration, 0.84 μg/mL) instead of VDAC.

Type B liposomes (circular dichroism): The stock SUV suspension was diluted with 1.5 volumes of TE buffer, and the resulting suspension was mixed with an equal volume of a suspension of 160 μg/mL VDAC in 2% β-OG/TE. This suspension was subjected to three freeze–thaw cycles (as above) and rapidly diluted into 3 volumes of TE buffer. The resulting clear suspension contained 1.5 mg/mL phospholipid, 20 μg/mL VDAC (i.e., 13.3 μg VDAC/mg lipid), and 0.25% β-OG.

Type C liposomes (patch clamping): Ten volumes of VDAC-containing type B liposomes were mixed with 1 volume of the stock SUV suspension, and the mixture was subjected to three freeze–thaw cycles. The resulting suspension of larger but more dilute vesicles contained 5 mg/mL phospholipid, 18 μg/mL VDAC (i.e., 3.6 μg VDAC/mg lipid), and 0.23% β-OG.

Liposome-swelling assays

0.5–5 μL of type A liposomes were diluted to 40 μL with TE buffer and mixed by vortexing. (This and all subsequent steps were done at room

temperature unless otherwise indicated.) The suspension was mixed well with 1 mL of TE buffer in a 1-cm path-length cuvette, and the turbidity was measured as A_{400} with a DU640 spectrophotometer (Beckman). After a stable baseline was recorded for ~5 min, 80 μL TE buffer was added to calibrate the effect of dilution. After another 5 min, 80 μL of 1 M sucrose (in TE buffer) was added to induce liposome shrinkage (increased A_{400}), which would be followed by reswelling (decreased A_{400}) if functional VDAC were present. Type C liposomes (16 μL) were also used to determine the effect of significantly larger protein:phospholipid ratios on the osmotic behavior of the liposomes. In general, reported experiments were done on at least two different days with different liposome preparations, with equivalent results obtained.

In experiments to determine the effects of elevated temperatures on VDAC function, 5-μL aliquots of type A liposomes were incubated for several minutes at 45–100° before or after mixing with 35 μL of TE buffer. These specimens were cooled to room temperature for at least 1 h before they were added to 1 mL of TE buffer for the light scattering experiments.

In experiments involving pH variations, 5-μL type A liposomes were diluted with 35 μL of 10 mM CAPS (pH 9–11) or 10 mM citrate (pH 5–3) buffers. Following incubation for at least 2 h, the suspensions were added to 1 mL of the same buffer for light-scattering experiments. To check reversibility of the result obtained at pH 3, KOH was gradually added to the liposome suspension until pH 6 was reached and the light-scattering experiment was repeated.

Patch-clamping experiments

The electrophysiological characteristics of purified VDAC were determined by voltage clamping of membrane patches excised from type C liposomes with glass microcapillary pipettes. Experiments were done in a symmetrical buffer (0.15 M KCl, 5 mM HEPES, pH 7.4), using procedures described by Kinnally et al. (1993). Voltage-clamp conditions were maintained with a model 3900 or 8900 amplifier (Dagan, Minneapolis, MN). Current and voltage data were digitized with a Neurocorder DR390 (NeuroData, New York, NY) and stored on video tape. Current data subsequently were low-pass filtered to 2 kHz and analyzed with Strathclyde Electrophysiological Data Analysis software (courtesy of J. Dempster, University of Strathclyde, UK). Open probabilities of channels were calculated as the ratio of time spent in open current levels over the total time (usually 30–60 s) as determined from total amplitude histograms.

Circular dichroism spectroscopy

Far-ultraviolet CD spectra of VDAC were measured at 25° with a J-720 spectropolarimeter (Jasco, Easton, MD) by use of quartz cuvettes of 0.05-cm path length (0.25-mL volume) in a temperature-controlled holder. Spectra were corrected for background by subtraction of spectra of identical suspensions without VDAC. Mean residue molar ellipticities, θ (deg cm^{-2} $dmol^{-1}$), were calculated based on protein concentrations determined as described above; a mean residue molecular weight of 106 was used.

The same VDAC fractions were used for CD as for the liposome swelling and bilayer experiments. All experiments reported were done at least twice on different protein preparations, with the experiments reported in Figs. 4–6 below done on the same protein fraction (i.e., one whose protein concentration was determined by amino-acid analysis as described above). Protein was acetone precipitated (as described above) from pooled column fractions and resuspended in TE buffer containing the indicated final concentrations of detergent (usually 2% β-OG) and indicated chemicals (salts, effectors, etc.). CAPS and citrate buffers were used to vary pH, as for the liposome swelling experiments. In some experiments, VDAC suspensions were heated for several minutes, then returned to 25° for at least 30 min before spectra were recorded.

Estimates of the secondary structure of VDAC based on CD spectra in 2% β-OG/TE were computed by two different algorithms: the variable-selection, single-value decomposition method of Manavalan and Johnson (1987) and the least-squares method of Yang et al. (1986). Reference spectra used with the variable-selection, single-value decomposition program were those of proteins with low to moderate α-helical content selected from among the 26 reference spectra provided with the program. The reference spectra used with the least-squares program were fixed (i.e., no selection was allowed).

RESULTS

Purification and biochemical characterization of VDAC

Following solubilization of fungal mitochondria with 4% LDAO, VDAC was found to bind to hydroxylapatite columns in low-salt buffer and to elute with 50 mM KCl, similar to the behavior of the mammalian protein (DePinto et al., 1989). As shown in Fig. 1, early fractions eluted with 50 mM KCl displayed a single major band in SDS-polyacrylamide gels at the M_r expected for VDAC (near 31,000), sometimes accompanied by a minor band at slightly higher M_r. Both bands were labeled in western blots by antibody against the amino terminus of fungal VDAC (Fig. 1), indicating that both correspond to VDAC. [Similar weak, slower-migrating VDAC bands are also observed in immunoblots of fungal mitochondria (Stanley et al., 1995) and may correspond to VDAC molecules with bound endogenous lipid, as observed with bacterial porins (Holzenberg et al., 1989)]. A second, minor, band also sometimes occurred at

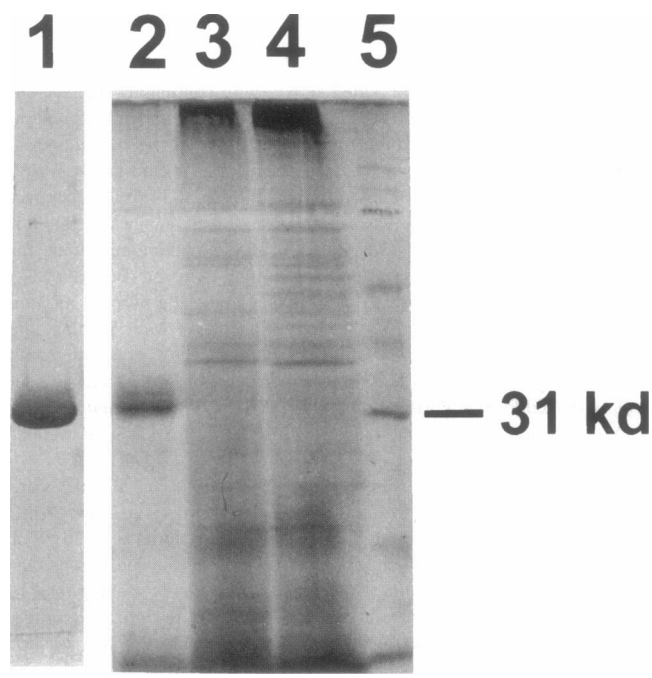

FIGURE 1 SDS-polyacrylamide gel electrophoresis and immunoblotting of VDAC isolated from *N. crassa* mitochondria. (*1*) Western blot of VDAC fraction eluted from hydroxyapatite column, probed with an antibody against the amino terminus of VDAC. (*2–5*) Silver-stained gel run with (*2*) the same VDAC fraction as for (*1*), (*3*) LDAO-solubilized mitochondrial protein fraction, (*4*) total mitochondrial protein, (*5*) molecular weight markers (band at 31,000 indicated).

the dye front on these gels ($M_r \leq 14{,}000$). This band was not labeled by anti-VDAC antibody and disappeared after routine concentration of the pooled fractions by centrifugation in Centricon 30 tubes.

Further confirmation that this protein fraction contains VDAC was provided by amino-acid analysis. As indicated in Table 1, the amino-acid composition is very close to that expected from the cDNA sequence of fungal VDAC (Kleene et al., 1987).

By use of this simple purification procedure, as much as 250 μg of pure VDAC could be obtained from 30-mg total mitochondrial protein, representing a yield of more than 0.8%, which compares favorably with yields obtained by other methods, e.g., less than 0.5% by Freitag et al. (1982).

Functional properties of purified VDAC

The purified VDAC fraction was reconstituted into phospholipid liposomes (as described in Material and Methods) and characterized by osmotic swelling and patch-clamping assays.

Liposome swelling

Type A liposomes, which contain ~20 ng VDAC/mg phospholipid, showed a characteristic biphasic response to addition of hyperosmotic sucrose: rapid shrinkage corresponding to fast efflux of water followed by a slower swelling phase (Fig. 2, curve a). The same liposomes prepared without VDAC, or with BSA (28 ng/mL phospholipid) instead of VDAC, or with thermally denatured VDAC (Fig. 2, curve b; see below), exhibited larger-scale osmotic shrinking and no reswelling. This is consistent with VDAC forming pores permeable to sucrose, which would reduce the initial osmotic response of the vesicles and allow subsequent equilibration of the sucrose concentrations inside and outside the vesicles (with accompanying water influx). It was found in other experiments (not shown) that an eightfold reduction in the concentration of VDAC eliminated the reswelling phase, whereas a 180-fold increase in VDAC concentration (corresponding to type C liposomes) rendered the vesicles osmotically unresponsive (i.e., no shrinkage phase). This concentration of purified fungal VDAC (3.6 μg/mg phospholipid) is the same as the concentration of rat-liver VDAC found by Linden et al. (1982) to make liposomes maximally permeable to sucrose. Although these experiments do not quantify the fraction of functional VDAC in these purified preparations, they indicate that these preparations have approximately the same pore-forming activity as those isolated by other protocols.

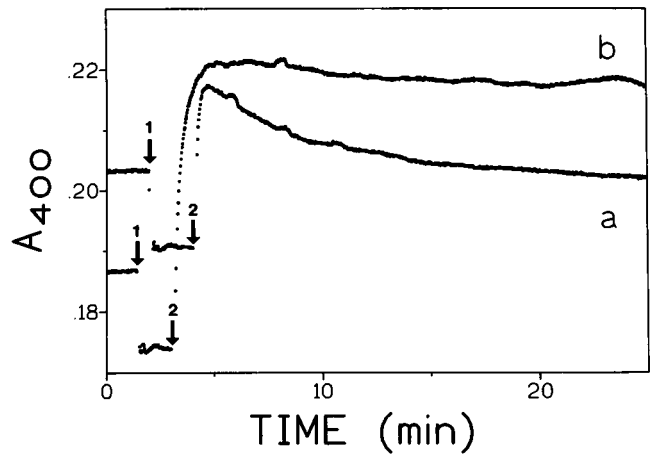

FIGURE 2 Osmotic response of liposomes reconstituted with fungal VDAC. Each curve shows an initial downward deflection, corresponding to dilution by an aliquot of iso-osmotic buffer at arrow 1, followed by a rapid upward deflection (liposome shrinkage) caused by addition of an equal aliquot of hyperosmotic sucrose (final concentration 0.08 M) at arrow 2. Curve (*a*) shows a slow reswelling of the liposomes, which presumably is due to VDAC-mediated influx of sucrose (followed by water). The reswelling phase is absent from curve (*b*), which corresponds to the same liposomes pretreated at 100° for 5 min.

TABLE 1 Amino-acid analysis of VDAC fraction

Amino acid	Measured	Expected*
Aspartic acid	30	33
Threonine	21	26
Serine	19	20
Glutamic acid	20	16
Proline	8	7
Glycine	29	25
Alanine	41	39
Valine	21	22
Methionine	2	2
Isoleucine	10	10
Leucine	23	19
Tyrosine	7	9
Phenylalanine	17	17
Histidine	7	8
Lysine	20	23
Arginine	6	5
Tryptophan	ND#	2
Cysteine	ND#	0

*Amino acid content based on cDNA sequence of Kleene et al. (1987).
#Not determined.

Ion conductance

The electrophysiological behavior of VDAC-containing liposomes (type C) was determined by patch-clamp experiments. Fig. 3 shows characteristic single-channel current traces obtained with a typical preparation and a graph of open probability versus voltage for the same specimen. Two transition sizes were observed with these preparations, 450 and 610 pS, corresponding to partial and total (or nearly total) closure of the channels. Although channel closures were seen at both negative and positive potentials, the voltage dependence was usually asymmetric; e.g., channels closed at smaller amplitude potentials for one polarity than for the other (Fig. 3). Asymmetric gating is not characteristic of VDAC in bilayers but has been observed with VDAC in liposomes (e.g., Wunder and Colombini, 1991).

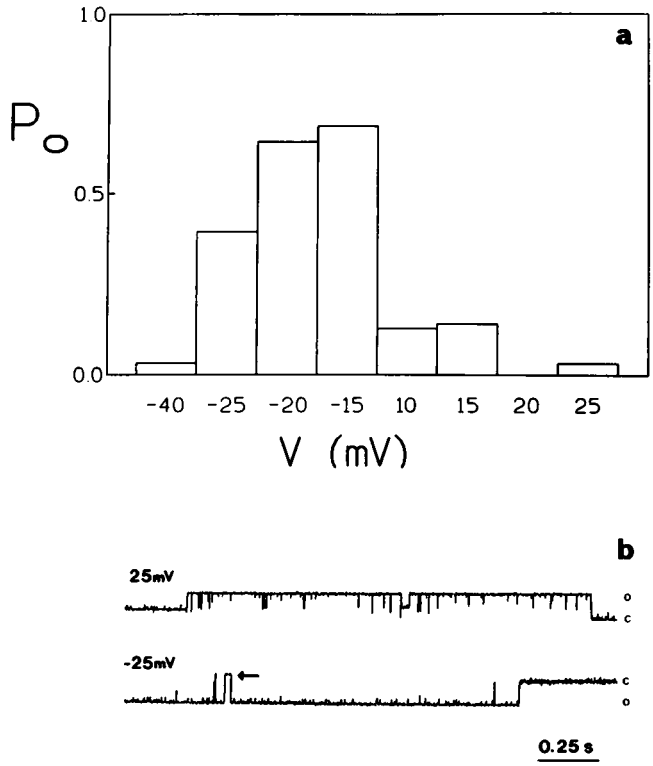

FIGURE 3 Electrophysiological characteristics of fungal VDAC reconstituted in liposomes. (*Top*) Voltage dependence of the open probability, P_o, of the channel. (*Bottom*) Typical current traces at transmembrane potentials of opposite polarity. The arrow points to a transition of ~600 pS.

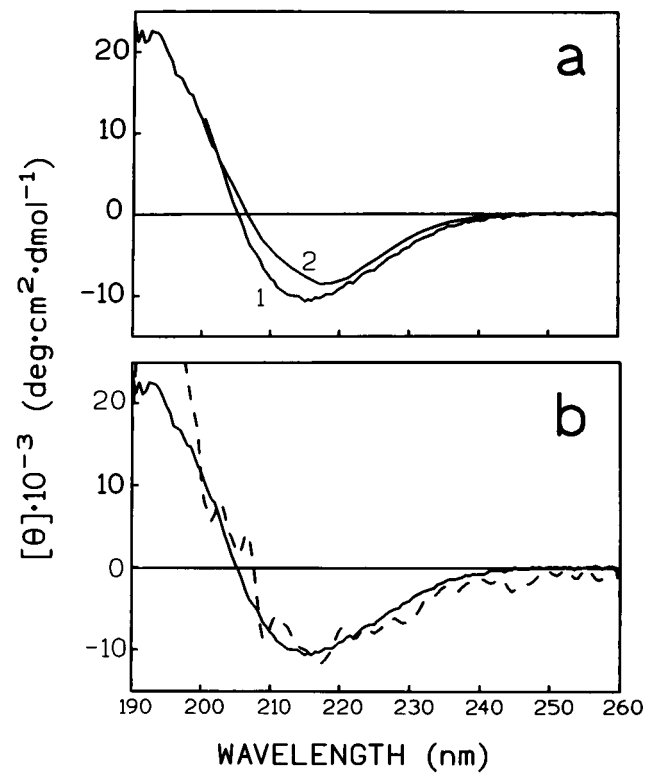

FIGURE 4 Far-ultraviolet CD spectra of fungal VDAC and bacterial porin. (*a*) Curve 1, fungal VDAC in 2% β-OG; curve 2, bacterial porin (OmpF) in 1% β-OG (data replotted from Markovic-Hously and Garavito, 1986). (*b*) Fungal VDAC in 2% β-OG (*solid curve*) and reconstituted in phospholipid liposomes (*dashed curve*).

Circular dichroism of fungal VDAC

CD spectra were recorded in the far ultraviolet from purified fungal VDAC in several different detergents and in liposomes (type B). With 1–2% LDAO or β-OG, reliable data could usually be recorded down to 180–190 nm. However, with Triton X-100 (0.1%) and liposomes, scattering limited the useful lower range of data collection to 200–210 nm.

The CD spectra of VDAC in 1–2% LDAO or β-OG in the range 190–260 nm were indistinguishable and comparable with those of bacterial porins in similar detergents (e.g., Tokunaga et al., 1979; Schindler and Rosenbusch, 1984; Markovic-Housley and Garavito, 1986; Worobec et al., 1988). Fig. 4 *a* compares the CD spectra of suspensions of fungal VDAC and *E. coli* OmpF in β-OG at room temperature and pH 7. The basic features are large positive ellipticity below 205 nm and a broad, less-intense minimum centered near 215 nm. Table 2 summarizes the characteristics of these spectra (and those of an "ideal" β-sheet protein) in terms of the wavelengths at which ellipticity equals zero ($\lambda_{crossover}$) and its minimum value (λ_{min}). The approximate content of secondary-structure elements (β-sheet, β-turn, α-helix, random coil) was computed from the spectrum of fungal VDAC in Fig. 4 by use of two different algorithms (see Materials and Methods), with the results summarized in Table 3. Both methods predict a β-sheet content for VDAC of ~60%, close to that of OmpF based on its x-ray crystal structure (56%; Cowan et al., 1992).

The CD spectra of fungal VDAC suspended in 0.1% Triton X-100 (not shown) and reconstituted in phospholipid liposomes (Fig. 4 *b*) were similar over their measurable range (i.e., down to ~200 nm) to those of VDAC in 1% or 2% β-OG and LDAO suspensions. This suggests that the conformation of VDAC in micelles of these detergents is similar to its pore-forming conformation in membranes. (The liposomes used for CD, osmotic swelling, and patch-clamping experiments were prepared by similar procedures from the same stock VDAC and SUV suspensions; see Materials and Methods.)

The CD spectrum of fungal VDAC in 2% β-OG was not noticeably altered by increased concentrations of salts such as KCl (up to 1 M) and $CaCl_2$ and $MgCl_2$ (up to 0.1 M). Also, no significant changes in the CD spectrum were

TABLE 2 Comparison of CD spectrum of VDAC with those of a bacterial porin and an ideal β-sheet protein

Protein	$\lambda_{crossover}$ (nm)	λ_{min} (nm)	$[\theta]_{min}$ (10^3 deg cm^{-2} dmol^{-1})
β-sheet*	204.5	214.0	−5.2
OmpF#	207.0	217.5	−8.5
VDAC	205.5	215.5	−10.0

*Yang et al. (1986).
#Markovic-Housley and Garavito (1986).

TABLE 3 Secondary structure of VDAC estimated from CD and predicted by models

Prediction	Secondary Structure α-helix (%)	β-sheet (%)	Other* (%)
Based on CD*			
pH 7, 25°	30 (7)	62 (63)	8 (31)
pH 4, 25°	28	38	34
pH 7, 65°	30	0	70
Based on models			
19-strand barrel§	–	81	–
12-strand barrel¶	–	51	–

*β-turn plus random coil.
#Estimates computed from CD spectra of fungal VDAC in 2% β-OG by method of Yang et al. (1986); values in parentheses computed from same data by method of Manavalan and Johnson (1987).
§Transmembrane β-sheet estimate for model of Forte et al. (1987).
¶Transmembrane β-sheet estimate for model of Blachly-Dyson et al. (1990).

caused by compounds known to alter the voltage dependence of the channel: 50 μM $AlCl_3$, 100 μM NADH, and 2 μM Koenig's polyanion (data not shown).

Effects of elevated temperature

Heating suspensions of fungal VDAC in 2% β-OG from 25° to 65° resulted in the progressive and irreversible changes in CD spectra illustrated in Fig. 5, namely, broadening of the minimum centered at 216 nm, a shift in $\lambda_{crossover}$ from 206 to ~195 nm, and an almost complete loss of positive ellipticity in the range 195–190. Heating to 100° caused total loss of ellipticity and absorbance, suggesting aggregation and precipitation of the protein. The CD changes at 65° were consistent with loss of most or all of the protein's β-sheet structure (Table 3). VDAC-reconstituted liposomes displayed irreversible loss of sucrose permeability when they were preheated above 65°, with total inhibition at 100° (Fig. 2). The irreversible loss of function at high temperature, also observed by Bathori et al. (1993) for liposome-reconstituted mammalian VDAC, suggests thermal denaturation of the channel protein. That the CD changes occurred at lower temperatures than inhibition of permeability suggests that the protein may be less stable in β-OG micelles than in phospholipid bilayers.

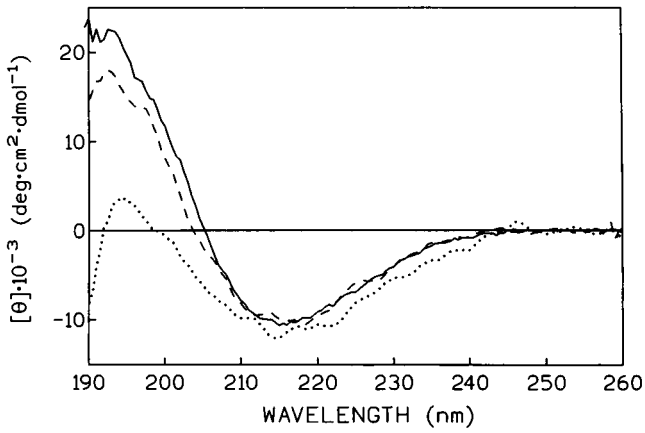

FIGURE 5 Effect of temperature on the CD spectrum of fungal VDAC. Spectra recorded from VDAC suspensions in 2% β-OG at 25° following incubation for 15 min at 45° (*dashed curve*) and 65° (*dotted curve*). The solid curve is the spectrum of a VDAC suspension in 2% β-OG kept at 25° (*curve 1*, Fig 4a).

Effects of variation of pH

Because the voltage-induced gating of the VDAC channel is pH dependent, the effects of varying pH on the CD spectra of purified fungal VDAC were examined. There were no appreciable changes in CD spectra of VDAC in 2% β-OG in the range pH 7 to 11 (data not shown). However, alterations in CD spectra were discernible below pH 5, as shown in Fig. 6 *a* and *b*. CD changes observed at pH 4–3 consisted of a broadening of the ellipticity minimum formerly centered at 216 nm and a resultant shift in $\lambda_{crossover}$ from 206 to ~200 nm, together with a decrease in positive ellipticity between 200 and 190 nm. The extent of the low-pH-induced CD changes varied somewhat between experiments (compare spectra in Figs. 6 *a* and *b*), but the loss of positive ellipticity below 200 nm was never as large as that observed at 65° (Fig. 5). In parallel experiments, the sucrose permeability of VDAC-containing liposomes was found to be greatly inhibited at pH 4 (Fig. 7). In marked contrast to the heat-induced effects, both the CD and permeability changes caused by lowering pH were almost fully reversed by restoring pH to 7 (Figs. 6 *b* and 7). Thus, the effects at low pH are consistent with a conformational change in VDAC that results in loss of sucrose permeability. Estimation of secondary structure from the CD spectrum of Fig. 6 *a* at pH 4 (Table 3) suggests that this conformational change corresponds to loss of approximately half of the β-sheet content of the open channel.

Effects of SDS; thermal stability of the SDS- and low-pH-induced states

As noted above, CD spectra of purified fungal VDAC in β-OG, LDAO, and Triton X-100 at pH 7 and room temperature were indistinguishable and were consistent with a high β-sheet content. At the same pH and temperature, the CD spectrum of VDAC in 1% SDS was markedly different, closely resembling that of VDAC at pH 3–4 in β-OG (Fig. 6 *c*).

Heating of VDAC in β-OG to 100° resulted in aggregation of the protein as noted above. However, it was found that suspensions of VDAC in SDS at pH 7 or in β-OG at pH 3 could be heated to 100° without precipitating and without additional changes in CD spectra (data not shown). These results suggest that the low-pH- and SDS-induced states of VDAC may be related and that they may represent a conformation that is more resistant to thermal denaturation than that at pH 7 in β-OG.

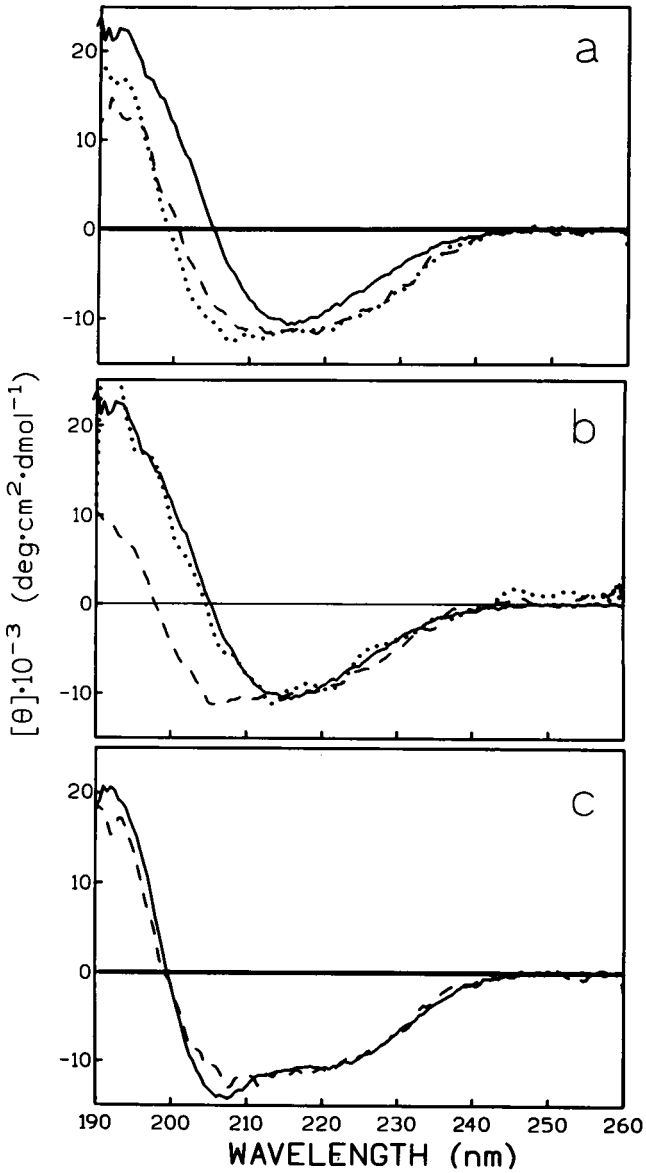

FIGURE 6 Effect of pH and SDS on the CD spectrum of fungal VDAC. (*a*) Spectra recorded from VDAC at pH 7.0 (*solid curve*), pH 4.0 (*dashed curve*), and pH 3.2 (*dotted curve*). (*b*) Spectra of VDAC at pH 7.0 (*solid curve*), pH 4.0 (*dashed curve*), and pH 6.0 after 1 h at pH 4.0 (*dotted curve*). (*c*) Spectra of VDAC in 1% SDS, pH 7.0 (*solid curve*) and in 2% β-OG, pH 4.0 (*dashed curve*). In (*a*) and (*b*), the spectrum of VDAC in 2% β-OG at pH 7 is from Fig. 4 *a*, curve 1.

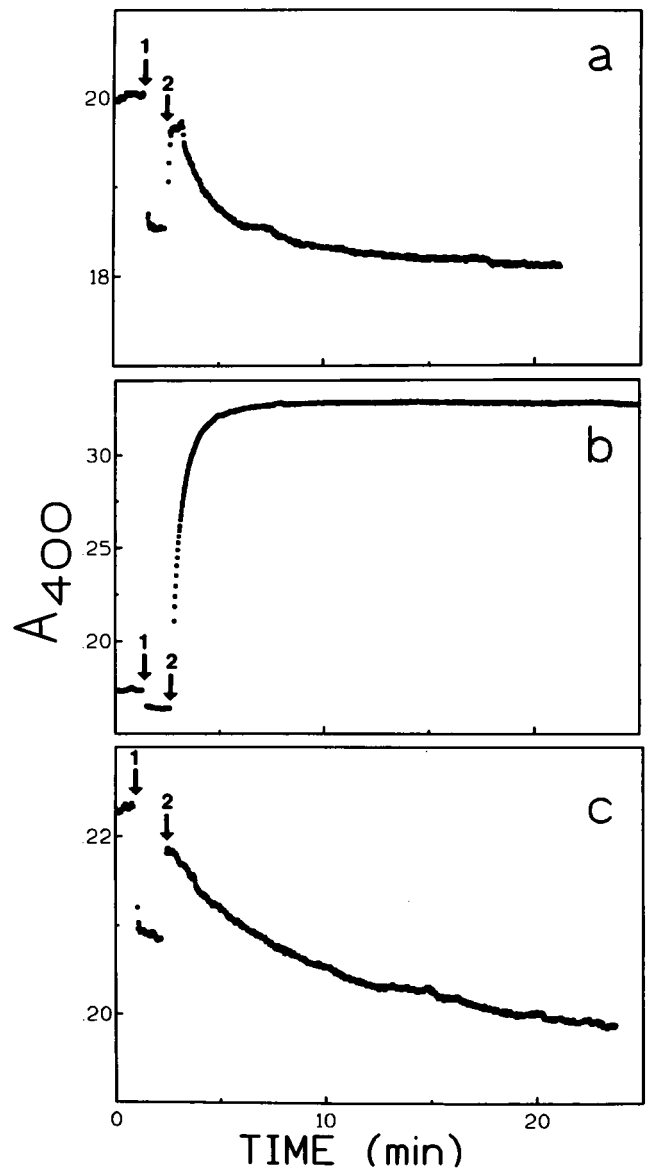

FIGURE 7 Effect of pH on sucrose permeability of fungal VDAC. Curves show the response of VDAC-containing liposomes to the addition of 0.08 M sucrose (same experimental conditions and procedures as in Fig. 2) for (*a*) liposomes at pH 7, (*b*) liposomes at pH 4, and (*c*) liposomes at pH 7 after incubation for 2 h at pH 4.

DISCUSSION

Although numerous structural models have been proposed for VDAC based on β-barrel motifs (e.g., Forte et al., 1987; Blachly-Dyson et al., 1990; DePinto et al., 1991; Rauch and Moran; 1994), this circular dichroism study provides the first direct, physical evidence that VDAC has a high β-sheet content. Current VDAC models vary widely in terms of the number of β-strands that might constitute the lumen-forming barrel. As indicated in Table 3, the β-sheet content predicted for VDAC based on its CD spectrum at pH 7 and 25° falls within the range expected for 12-strand (Blachly-Dyson et al., 1990) and 19-strand (Forte et al., 1987) β-barrel models. However, inasmuch as these CD-based predictions are only estimates, they cannot be used to distinguish among the different folding models.

The CD experiments on fungal VDAC in β-OG micelles, correlated with osmotic swelling experiments on VDAC-containing liposomes, indicate that the mitochondrial channel protein undergoes a reversible conformational change at pH 4, involving partial loss of β-sheet content. A related conformation, which, like the low-pH state, appears to be resistant to thermal denaturation, is induced in VDAC by the detergent SDS at pH 7. It is unclear whether this lower

β-sheet conformation has any functional significance. Peng et al. (1992) have proposed a model for closure of VDAC that involves removal of transmembrane strands from the putative β-barrel, thus reducing the pore's diameter and permeability. That low pH concomitantly induces in VDAC reversible decreases in sucrose permeability and β-sheet content might be considered to support such a closure mechanism. Lowering pH to 3–4 has been reported by Mirzabekov and Ermishkin (1989) to decrease the voltage needed to induce partial closure of VDAC in bilayers. However, low pH alone does not induce the partially closed state of VDAC characterized by Peng et al. (1992). In addition, this voltage-induced substate is expected to be permeable to sucrose, albeit less so than the fully open state. Thus, it is unlikely that the conformation induced in VDAC by low pH corresponds to the usually observed voltage-induced, partially closed state of the channel.

Earlier studies indicate that bacterial porins undergo a conformational change that may be related to that observed with VDAC, albeit under different combinations of conditions. For example, reversible changes in CD spectra such as those observed with VDAC in β-OG at pH 4 or in SDS at pH 7 also have been observed with bacterial porins, but only in SDS and only after exposure to either low pH (Schindler and Rosenbusch, 1984; Markovic-Housley and Garavito, 1986) or heat (Tokunaga et al., 1979; Worobec et al., 1988; Chevalier et al., 1993). These bacterial porins (unlike VDAC) normally occur as trimeric complexes that are stable in SDS at room temperature. Only after dissociation of the trimers into monomers by heating or low pH are the CD changes observed. OmpA, a monomeric, non-pore-forming β-barrel protein in the outer membrane of *E. coli*, displays CD changes during refolding (from a urea-denatured state) and membrane insertion (Surrey and Jahnig, 1995) that are similar to those displayed by VDAC in β-OG when pH is raised from 4 to 6 (Fig. 6 *b*). This raises the possibility (currently under examination) that the low-pH conformation may represent a folding intermediate on the pathway from VDAC's water-soluble form (following synthesis on cytoplasmic ribosomes) to outer-membrane insertion and pore formation.

Aside from low pH, other known effectors of the voltage dependence of VDAC did not appreciably alter the CD spectrum of the protein. The absence of effects of high pH and aluminum on VDAC's CD spectrum was not surprising. These conditions decrease voltage-dependent gating of VDAC, presumably by altering gating charges (Bowen et al., 1985; Dill et al., 1987), and are not thought to cause major conformational changes. Likewise, although NADH induces a steeper voltage response in VDAC (Zizi et al., 1994), it makes the channel less likely to close at near-zero transmembrane potentials. Only Koenig's polyanion is expected to induce a transition to a closed state in the absence of a transmembrane potential, based on its effects on the permeability of mitochondrial outer membranes (Benz et al., 1988) and VDAC-containing liposomes (Colombini et al., 1987). That the polyanion does not alter the CD spectrum of VDAC in β-OG suggests either that polyanion-induced closure does not involve major changes in VDAC's secondary structure or that the effects of the polyanion are mitigated in detergent suspension.

We thank Dr. Patrick Van Roey and Dr. Robert MacColl, director of the Wadsworth Center's biochemistry core facility, for advice and assistance with aspects of protein isolation and CD spectroscopy and Dr. Li-Ming Chen of the Wadsworth Center's protein chemistry core facility for performing the amino-acid analysis. This research was supported by grants MCB-9219353 and MCB-9506113 from the National Science Foundation.

REFERENCES

Bathori, G., M. Sahin-Toth, A. Fonyo, and E. Ligeti. 1993. Transport properties and inhibitor sensitivity of isolated and reconstituted porin differ from those of intact mitochondria. *Biochim. Biophys. Acta.* 1145: 168–176.

Benz, R., L. Wojtczak, W. Bosch, and D. Brdiczka. 1988. Inhibition of adenine nucleotide transport through the mitochondrial porin by a synthetic polyanion. *FEBS Lett.* 231:75–80.

Blachly-Dyson, E., S. Z. Peng, M. Colombini, and M. Forte. 1990. Selectivity changes in site-directed mutants of the VDAC ion channel: structural implications. *Science.* 247:1233–1236.

Bowen, K. A., K. Tam, and M. Colombini. 1985. Evidence for titratable gating charges controlling the voltage dependence of the outer mitochondrial channel, VDAC. *J. Membr. Biol.* 86:51–59.

Chevalier, G., H. Doclohier, D. Thomas, E. Shechter, and H. Wroblewski. 1993. Purification and characterization of protein H, the major porin of *Pasteurella multocida*. *J. Bacteriol.* 175:266–276.

Colombini, M. 1979. A candidate for the permeability pathway of the outer mitochondrial membrane. *Nature (London).* 279:643–645.

Colombini, M. 1980. Structure and mode of action of a voltage dependent anion-selective channel (VDAC) located in the outer mitochondrial membrane. *Ann. N.Y. Acad. Sci.* 341:552–563.

Colombini, M. 1994. Anion channels in the mitochondrial outer membrane. *Curr. Top. Membr.* 42:73–101.

Colombini, M., C. L. Yeung, J. Tung, and T. König. 1987. The mitochondrial outer membrane channel, VDAC, is regulated by a synthetic polyanion. *Biochim. Biophys. Acta.* 905:279–286.

Cowan, S. W., T. Schirmer, G. Rummel, M. Steiert, R. Ghosh, R. A. Pauptit, J. N. Jansonius, and J. P. Rosenbusch. 1992. Crystal structures explain functional properties of two *E. coli* porins. *Nature (London).* 358:727–733.

De Pinto, V., R. Benz, and F. Palmieri. 1989. Interaction of non-classical detergents with the mitochondrial porin. A new purification procedure and characterization of the pore-forming unit. *Eur. J. Biochem.* 183: 179–187.

De Pinto, V., G. Prezioso, F. Thinnes, T. A. Link, and F. Palmieri. 1991. Peptide-specific antibodies and proteases as probes of the transmembrane topology of the bovine heart mitochondrial porin. *Biochemistry.* 30:10191–10200.

Dill, E. T., M. J. Holden, and M. Colombini. 1987. Voltage gating in VDAC is markedly inhibited by micromolar quantities of aluminum. *J. Membr. Biol.* 99:187–196.

Forte, M., H. R. Guy, and C. A. Mannella. 1987. Molecular genetics of the VDAC ion channel: structural model and sequence analysis. *J. Bioenerg. Biomembr.* 19:341–350.

Freitag, H., W. Neupert, and R. Benz. 1982. Purification and characterization of a pore protein of the outer mitochondrial membrane from *Neurospora crassa*. *Eur. J. Biochem.* 123:629–639.

Guo, X. W., P. R. Smith, B. Cognon, D. D'Arcangelis, E. Dolginova, and C. A. Mannella. 1995. Molecular design of the voltage-dependent, anion-selctive channel in the mitochondrial outer membrane. *J. Struct. Biol.* 114:41–59.

Holden, M. J., and M. Colombini. 1993. The outer mitochondrial membrane channel, VDAC, is modulated by a protein localized in the intermembrane space. *Biochim. Biophys. Acta.* 1144:396–402.

Holzenberg, A., A. Engel, R. Kessler, H. J. Manz, A. Lustig, and U. Aebi. 1989. Rapid isolation of OmpF Porin-LPS, complexes suitable for structure-function stuides. *Biochemistry.* 28:4187–4193.

Kinnally, K. W., D. B. Zorov, Yu. Antonenko, S. Snyder, M. W. McEnery, and H. Tedeschi. 1993. Mitochondrial benzodiazepine receptor linked to inner membrane ion channels by nM actions of ligands. *Proc. Natl. Acad. Sci. USA.* 90:1374–1378.

Kleene, R., N. Pfanner, R. Pfaller, T. Link, W. Sebald, W. Neupert, and M. Tropschug. 1987. Mitochondrial porin of *Neurospora crassa*: cDNA cloning, in vitro expression and import mitochondria. *EMBO J.* 6:2627–2633.

Linden, M., P. Gellerfors, and B. D. Nelson. 1982. Purification of a protein having pore forming activity from the rat liver mitochondrial outer membrane. *Biochem. J.* 208:77–82.

Manavalan, P., and W. C. Johnson, Jr. 1987. Variable selection method improves the prediction of protein secondary structure from circular dichroism. *Anal. Biochem.* 167:76–85.

Mannella, C. A. 1982. Structure of the outer mitochondrial membrane: ordered arrays of porelike subunits in outer-membrane fractions from *Neurospora crassa* mitochondria. *J. Cell Biol.* 94:680–687.

Mannella, C. A., M. Forte, and M. Colombini. 1992. Toward the molecular structure of the mitochondrial channel, VDAC. *J. Bioenerg. Biomembr.* 24:7–19.

Mannella, C. A., X. W. Guo, and B. Cognon. 1989. Diameter of the mitochondrial outer membrane channel: evidence from electron microscopy of frozen-hydrated membrane crystals. *FEBS Lett.* 253:231–234.

Mannella, C. A., A. F. Neuwald, and C. E. Lawrence. 1996. Detection of likely transmembrane beta-strand regions in sequences of mitochondrial pore proteins using the Gibbs sampler. *J. Bioenerg. Biomembr.* 28: 163–169.

Markovic-Housley, Z., and R. M. Garavito. 1986. Effect of temperature and low pH on the structure and stability of matrix porin in micellar detergent solutions. *Biochim. Biophys. Acta* 869:158–170.

Mirzabekov, T. A., and L. N. Ermishkin. 1989. The gate of mitochondrial porin channel is controlled by a number of negative and positive charges. *FEBS Lett.* 249:375–378.

Neuwald, A. F., J. S. Liu, and C. E. Lawrence. 1995. Gibbs motif sampling: detection of bacterial outer membrane protein repeats. *Protein Sci.* 4:1618–1632.

Peng, S., E. Blachly-Dyson, M. Forte, and M. Colombini. 1992. Large scale rearrangement of protein domains is associated with voltage gating of the VDAC channel. *Biophys. J.* 62:123–135.

Pfaller, R., and W. Neupert. 1987. High-affinity binding sites involved in the import of porin into mitochondria. *EMBO J.* 6:2635–2642.

Rauch, G., and O. Moran. 1994. On the structure of mitochondrial porins and its homologies with bacterial porins. *Biochem. Biophys. Res. Comm.* 200:908–915.

Schindler, M., and J. P. Rosenbusch. 1984. Structural transitions of porin, a transmembrane protein. *FEBS Lett.* 173:85–89.

Stanley, S., J. A. Dias, D. D'Arcangelis, and C. A. Mannella. 1995. Peptide-specific antibodies as probes of the topography of the voltage-gated channel in the mitochondrial outer membrane of *Neurospora crassa*. *J. Biol. Chem.* 270:16694–16700.

Surrey, T., and F. Jahnig. 1995. Kinetics of folding and membrane insertion of a beta-barrel membrane protein. *J. Biol. Chem.* 270: 28199–28203.

Tokunaga, M., H. Tokunaga, Y. Okajima, and T. Nakae. 1979. Characterization of porins from the outer membrane of *Salmonella typhimurium*. 2. Physical properties of the functional oligomeric aggregates. *Eur. J. Biochem.* 95:441–449.

Weiss, M. S., T. Wacker, J. Weckesser, W. Welte, and G. E. Schulz. 1990. The three-dimensional structure of porin from *Rhodobacter capsulatus* at 3 Å resolution. *FEBS Lett.* 267:268–272.

Worobec, E. A., N. L. Martin, W. D. McCubbin, C. M. Kay, G. D. Brayer, and R. E. W. Hancock. 1988. Large-scale purification and biochemical characterization of crystallization-grade porin protein P from *Pseudomonas aeruginosa*. *Biochim. Biophys. Acta.* 939:366–374.

Wunder, U. R., and M. Colombini. 1991. Patch clamping VDAC in liposomes containing whole mitochondrial membranes. *J. Membr. Biol.* 123:83–91.

Yang, J. T., C.-S. Wu, C., and H. M. Martinez. 1986. Calculation of protein conformation from circular dichroism. *Meth. Enzymol.* 130:208–269.

Zizi, M., M. Forte, E. Blachly-Dyson, and M. Colombini. 1994. NADH regulates the gating of VDAC, the mitochondrial outer membrane channel. *J. Biol. Chem.* 269:1614–1616.